



The effect of composite boring bars on vibration in machining process

S. Ghorbani¹ · V. A. Rogov¹ · A. Carluccio² · P. S. Belov¹

Received: 9 May 2019 / Accepted: 13 August 2019 / Published online: 27 August 2019
© Springer-Verlag London Ltd., part of Springer Nature 2019

Abstract

One of the challenges of machining process is to improve the quality of machined surface by reducing the vibration of cutting tools. The research aims to suppress vibration using composite boring bars with an enhanced damping capacity. A new design of boring bars with different cross-sections is considered. Static and dynamic behavior of the proposed tools is investigated. A mathematical model for determining the eigenfrequency is proposed, and it is compared with computer simulation and experimental results. The validity of the proposed models is verified by conducting experimental machining tests in order to study the changes in vibro-acoustic signals depending on the cross-sections of the toolholder. The results show that the composite material significantly improves damping of boring bars, which leads to a reduction in the vibration compared to conventional boring bars.

Keywords Damping · Epoxy granite · Vibration · Machining process · Vibro-acoustic signal

1 Introduction

At present, experts working in engineering face a number of important tasks, such as improving the competitiveness and technological level of the cutting tool and metalworking equipment and reducing the cost of metalworking, e.g., turning, milling, and boring operations. One of the main methods to reduce the production cost is to increase the productivity of metalworking, especially boring operations, which can be done by increasing the cutting speed and using more advanced designs of cutting tools. The main focus in the development of modern engineering production is automation, which puts high demands on the machining tools to increase productivity. The implementation of automation in the processing chain of the production intensifies not only the cutting conditions, but ranges of drive regulation, power, and speed of the moving parts of machines, and the load acting on them. This causes

considerable vibrations and thermal growth, which adversely affects accuracy and leads to an accelerated cutting tool wear [1–3]. Vibrations occurring in a machining process are dangerous, especially during the finishing operations while working with high-precision machine tools [4, 5].

Considerable research has been conducted to find out how to avoid vibrations occurring during a machining process. Such research first started at the beginning of the twentieth century by Taylor [6], and then in the 1940s, Arnold [7] studied cutting tool vibrations based on experimental turning operation. Later, many efforts were made by Tobias and Fishwick [8], Tlustý and Poláček [9], Smith [10], Merritt [11], and Altintas and Budak [12] to identify the chatter problem for the machining productivity. Machine vibrations are transferred to the workpiece through the tool and fixtures, so that the surface quality is significantly reduced. The vibration problem during boring operation is increasingly more significant because for this operation, a flexible cutting tool is used. Different authors focused their attention on analytical and experimental studies of the boring bar dynamic. Parker [13] studied the stability of a cantilever boring bar, represented by a simple two-degree-of-freedom mass-spring-damper system, in order to identify the effect of coupling between the modes on the vibration behavior during a machining process. Zhang and Kapoor [14] derived an analytical form of tool motion to predict the boring bar chatter during a machining process. They also experimentally determined the stability

✉ S. Ghorbani
ghorbani_s@pfur.ru

¹ Department of Mechanical and Instrumental Engineering, Academy of Engineering, Peoples' Friendship University of Russia, No. 3, Ordjanikidze, Moscow, Russia

² Department of Russian Language and Teaching Methods, Peoples' Friendship University of Russia, No. 6, Miklukho-Maklaya, Moscow, Russia

limit of width of the cut and compared it with the results of the predicted values. Rao et al. [15] provided a new dynamic boring force model that considers the chip cross-sectional area under dynamic conditions. Andren et al. [16] identified the boring bar vibration properties using the Euler–Bernoulli beam model and compared it with the time-series approach. Sortino et al. [17, 18] studied the process damping stability in the internal finish turning a hybrid dynamic model of the tooling system based on finite element beams and empirical models. They claimed that the experimental damping values mainly depended on the ratio of the boring bar overhang to the bar external diameter and on the boring bar material. Another strategy to improve the dynamic behavior of the boring bar is analyzing the influence of the clamping condition [19] and the geometry of the cutting insert on the cutting force [20–23].

Using a standard tool in machines cannot provide the desired result, since the tool, as a final point of contact of the machine-tool-workpiece having a nanometric accuracy, should not only absorb the vibrations transmitted from the machine, but should also have a minimum temperature expansion during machining. The production of such a tool cannot be imagined without the use of modern construction materials and advanced technologies [24], since the dynamic stiffness and eigenfrequency of boring bars depend on damping, static stiffness [25], and on the specific stiffness of the boring bar material [26]. Therefore, materials used for boring bars should possess high static stiffness as well as damping properties.

Passive and active damping mechanisms are another method that can control the vibration level. Although active dampers are more effective in vibration suppression, they are very expensive since they are complex in design and they consume high external power [4]. In contrast, passive damping does not need external energy and it is simpler and more economical [27, 28]. There are only a few intrinsic damping mechanisms in metals, which are effective in a wide range of amplitudes, frequencies, and temperatures [29]. Some works on improving the damping behavior of the boring bar are briefly summarized below. Most of them are based on the creation of high heterogeneity of boring bars with a soft component responsible for a high damping capacity.

Nagano et al. [30] designed four types of composite boring bars, having different shaped steel cores, based on pitch-based carbon fiber reinforced plastic, in order to increase chatter resistance of the tool structure compared to the conventional steel and cemented carbide bars. Ema and Marui [31] used three types of impact dampers in boring bars. Impact dampers consist of free mass and clearance. A ring-shaped free mass was equipped on the flank face or the top face of a boring tool using a bolt and a supplementary sleeve. The other one was equipped by a ring-shaped free mass along the center axis of a boring tool shank. The authors stated that damping capacity of boring bars was improved and chatter vibration was suppressed effectively. Hwang et al. [32] developed a clamping

part with a metal core or a sleeve inserted in the composite body at the clamping part and investigated the clamping effects on the dynamic characteristics of the composite boring bar in order to increase the eigenfrequency and damping of the structures using a finite element analysis and impulse response tests. Lee et al. [33, 34] stated that using carbon fiber epoxy composite material in the boring bar has suppressed vibration in metal cutting and improved the dynamic stiffness about 30% in comparison with tungsten carbide boring bar. Miguelez et al. [35] improved the behavior of boring bars against chatter using a passive dynamic vibration absorber taking into consideration mass, stiffness, damping, and position as the absorbers parameters to construct the stability-lobes diagram. Saffury and Altus [36] analyzed a viscoelastic beam to suppress the vibration of turning bars during machining operations and compared to the common dynamic vibration absorber. Rubio et al. [37] suppressed chatter in the boring bar by selecting an optimum parameter of a passive vibration absorber attached to a boring bar.

The objective of the present work is to develop boring bars with an enhanced damping capability using epoxy granite to suppress chatter during a machining process. The application of composite materials such as epoxy granite can provide high dynamic stiffness and decrease the eigenfrequency of the boring bar due to their better specific properties of strength and stiffness as well as high damping in comparison with steel and cast iron [38, 39]. The static, dynamic, and computer investigations of the proposed tools are carried out. The relationships between damping capacities of the modified boring bars and the frequency response of the vibro-acoustic signal are determined.

2 Materials and methods

2.1 The object of study

The object of the study is a boring bar, model S32X-PCLNR 12-Bh 12, made of a hardened steel (AISI 5140), and with a rhombic insert. The boring bar cross section is circular with $\varnothing 32$ mm and length of 213 mm. It should be mentioned that geometrical requirements of the boring bar are related to degrading vibrations, influencing on surface quality, tool durability, and productivity [35].

In this study, in order to increase the damping capability of the boring bar, passive damping mechanism is used, which is based on changing boring bars performance against vibration by improving the design of the boring bar or application of material with high damping capability in the structure of the boring bars to dissipate extra energy [4]. Damping capacity in eleven boring bars with different cross section is investigated. One of them remains as the conventional boring bar for comparison (cross section No. 0 in Fig. 1a); in ten others, the

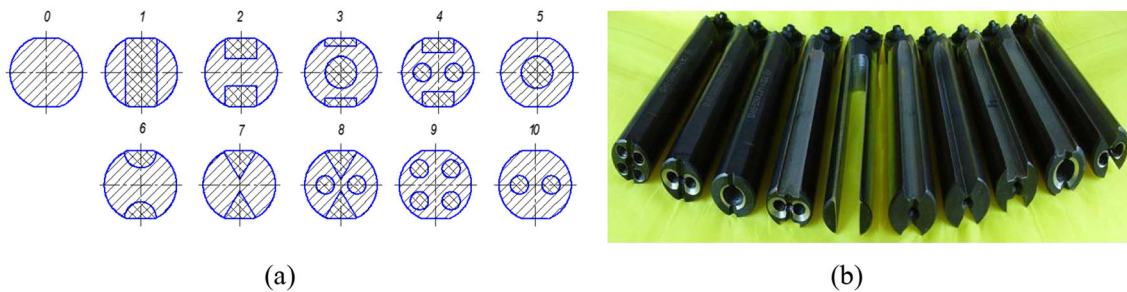


Fig. 1 **a** Cross-sectional shapes of the modified boring bars. **b** The modified boring bars

longitudinal grooves with different cross-sectional shapes for the length of 160 mm are made (Fig. 1b). These grooves are used to fill up toolholders with composite material. The cross section of toolholder, reinforced by composite material, largely changes the static and dynamic stiffness of the tool.

Thus, new cutting tools are designed and made such that they are simple in design, and they have a variety of mass combination of metal skeleton (steel “skeleton”) and filler (composite material), contact area of the composite material and the steel, as well as moments of inertia of the cross sections. The epoxy granite is used as a composite material, which is a reinforced composite material based on epoxy binder (thermoset resins) and fillers in the form of rubble and fine powder made of high-strength granite and gabbro-diabase. The epoxy granite belongs to the category of a polymer concrete and possesses good mechanical properties [38]. Epoxy granite is applied in different fields such as machineries, construction in structural materials, where high damping, physical, mechanical, durability, chemical, thermal properties, and efficiency in the product preparation are required [39]. Table 1 shows the physical and mechanical characteristics of epoxy granite [38, 39]. Before filling the grooves by epoxy granite, they were carefully degreased and dried. The following mixture was prepared for filling the grooves by epoxy granite. The fillet was granite with a grain size of less than 0.5 mm. The epoxy resin solution ED-20 4.5–7.4%, active diluent 0.8–2%, 1.6–2.3% of an amine hardener are used as a composite. Curing process took place for 24 h at standard conditions.

Table 1 Physical and mechanical characteristics of epoxy granite

Parameter	Epoxy-granite
Density (kg/m ³)	2400–2600
Strength stress (MPa)	
Compression	150–160
Tensile	15–20
Elasticity module (MPa*10 ⁻⁴)	3.5–4.0
Poisson's ratio	0.25–0.40
Thermal conductivity (W/(m*K))	1.7–1.75
Linear expansion coefficient (1/°C)	(12–16)*10 ⁻⁶

The adhesive not only helps the steel to join the composite shank, but also can increase the damping of the boring bar through the constrained damping mechanism [40].

The moment of inertia of the boring bars, as one of the main physical characteristics affecting stiffness of toolholder and damping capability, is determined by the ratio of geometric parameters for which it is defined. In this case, the toolholders have inhomogeneous structures, so the calculation of the moment of inertia should be made separately for the metal body and the filler. The moment of inertia for the conventional and proposed boring bars are determined using Eqs. (1) and (2). Quantitative value of volume fraction of epoxy granite in the modified boring bars and the contact area between metal and the fillet (epoxy granite) have a direct impact on the damping capability of boring bars. The amount of volume fraction of epoxy granite can be defined as a volume of the toolholder filled with epoxy granite and the contact area taken as a contact length of the metal and epoxy granite multiplied by length of the toolholder filled with epoxy granite plus contact area between metal and epoxy granite at the end of the toolholder. The obtained data are presented in Table 2.

Table 2 Summary of numerical characteristics of the boring bars reinforced by epoxy granite

No. of cross section	Contact area between metal and epoxy granite, mm ²	Volume fraction of epoxy granite, mm ³	Moment of inertia of toolholder, mm ⁴	Maximum strength, MPa
0	0	0	51445	190.430
1	9538	66880	19945	268.872
2	9850	40000	22181	229.286
3	13530	40000	32257	222.348
4	16600	44800	25275	224.270
5	7034	24480	49561	207.833
6	7046	27556	16018	207.833
7	8982	29120	30270	216.48
8	17082	45120	29868	224.450
9	16200	32000	40841	203.124
10	8100	16000	51043	196.570

$$Y_x = \pi d^4 / 64, \tag{1}$$

$$Y_{x_1} = Y_{x_2} + PY^2, \tag{2}$$

where Y_x represents the moment of inertia of the conventional boring bar, d is the diameter of the toolholder, Y_{x_1} is the moment of inertia of the modified boring bar, Y_{x_2} is the centrifugal inertia, P is the area of the cross section, and y is the coordinate of the center of gravity.

One of the important processes in boring bar design is the determination of their strength. For this reason, the boring bar is considered to be a cantilever beam for which the classical methods of material strength is applied using the Eqs. (3) and (4):

$$\sigma < \sigma_{per}, \tag{3}$$

$$\sigma = M/W, \tag{4}$$

where σ represents the maximum strength of the boring bar, σ_{per} is the permissible strength of the boring bar which is 400 MPa for the material AISI5140, M is the bending moment, W is the moment of resistance of the cross section of the tool holder.

The results of the strength calculation are represented in Table 2. As can be seen from the Table 2, the maximum strength values of all boring bar are less than the permissible one. Therefore, the modified boring bars have enough strength during machining process.

2.2 Analytical model

It is known that tool life depends not only on the amplitude, but also on the frequency of vibrations arising during cutting process. The so-called “high vibration” during cutting is excited at the frequencies of cutting tool’s eigenfrequencies or close to them [41]. Theoretical analysis of vibration frequency can be simplified, if the form of vibration corresponding to the first harmonic of the eigenfrequencies spectrum is considered. During the analysis, the following assumptions have been made: the cross section of the toolholder is constant along the length; the weight of the toolholder is uniformly distributed along its length. It is known, that the tool tip displacement (Fig. 2a) is calculated by the following equation of elasticity [42]:

$$Z_i = PLy_i^2(3-y_i/2)(1/6EJ^2), \tag{5}$$

where z_i represents the displacement of the i -th section in Z direction, P is the cutting force in z direction (N), L is the length of the beam (tool overhang) (mm), y_i is the distance of the i -th section of the seal, E is elastic modulus of the toolholder and J is moment of inertia of toolholder cross section.

In accordance with the assumptions made, when considering the first harmonic of the toolholder vibrations, (namely,

this harmonic has the highest amplitude of the relative vibration frequency affecting the tool life), it can be shown that the dynamic system of the toolholder can lead to a single-mass model. Therefore, the real toolholder with uniformly distributed mass along the length is replaced to the single-mass system as a weightless elastic beam with concentrated mass (M) at its end (Fig. 2b).

The length and stiffness of the beam are equal to the length and the stiffness of the actual toolholder.

We assume that the equation for tool tip displacement is known as:

$$Z = f(y), \tag{6}$$

where z represents the displacement of the toolholder section during bending and y is the distance of this section from the fixed part.

The toolholder mass is calculated from the equal conditions of kinetic energies in the vibrational motion of the actual toolholder and the computational model:

$$\left(Mz_L^2/2 \right) = \int_0^L \left(bh\gamma \dot{z}^2(y)dy/2 \right), \tag{7}$$

where M represents the mass of the toolholder, \dot{z} is the speed of the last point during vibration (m/s), b is the width of the toolholder cross-section, h is the height of the toolholder cross section, γ is the density of material of the toolholder and $\dot{z}(y)$ is the speed of the section dy in the vibration process. Since the eigenfrequency (f_0) of the real toolholder and calculated model (according to the condition) are equal, therefore, the speed of amplitude could be written as:

$$\dot{z}^2(y) = z^2(y)f_0^2, \text{ and } \dot{z}_L^2 = z_L^2f_0^2, \tag{8}$$

Substituting Eq. (8) into Eq. (7) and replacing integration by summation of small sections of Δy , after appropriate transformations, the following expression is achieved:

$$M = \int_0^L (bh\gamma z^2(y)dy/2) = M_0 \sum_{i=1}^n (Z_i^2/Z_L^2), \tag{9}$$

$$M_0 = bhL\gamma, \tag{10}$$

where M_0 represents the mass of the unfixed part of the toolholder, Z_i is the displacement of the midsection (Δy) of the holder, n is the number of calculated sections of the toolholder ($n = L/\Delta y$).

Substituting the expression $Z(y)$ and Z_L from Eq. (5) into Eq. (9) and after integrating, the next expression is obtained:

$$M = (M_0/4L^5) \int_0^L (3y^2 - (y^3/L))^2 dy = 0.2357M_0, \tag{11}$$

Using the well-known expression for the calculation of the eigenfrequency (f_0) for single-mass system with the linear stiffness it can be written:

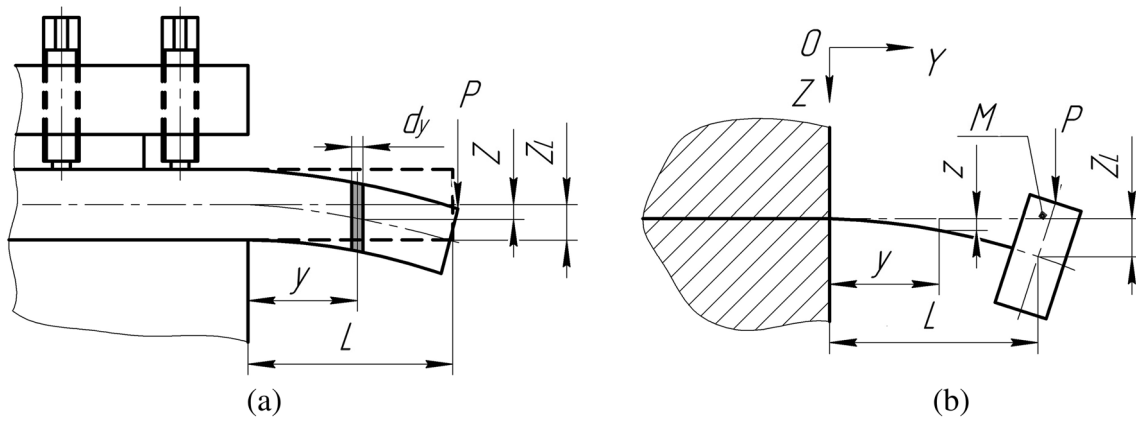


Fig. 2 Analytical beam model of boring bar. a 3D-model of the cutting tool. b) Single-mass model of the cutting tool

$$f_0 = (1/2\pi)\sqrt{C/M} = (1.03h/\pi L^2)\sqrt{E/\gamma}, \tag{12}$$

where C represents the stiffness of toolholder, i.e., the inverse quantity of the displacement of its free end in a single action force (N/m).

By substituting the modulus of elasticity and density for steel toolholders into the Eq. (12), it can be simplified as:

$$f_0 = (8.505h/L^2)10^5, \tag{13}$$

2.3 Computer simulation of boring bars

To determine the physical and mechanical properties of the modified boring bars and to identify the most rational design for vibration damping, 3D models of the boring bars are created with cross section according to the Fig. 1. The computer analysis is carried out based on the finite element method using Solidworks Simulation. To provide computer analysis, the materials of the models, constraints, clamping force, and cutting force are defined similar to the real boring bar. Material of the toolholder is hardened steel (AISI 5140); cutting insert is made of hard alloy (CT35M) and properties of epoxy granite are according to the Table 1. The meshing was carried out by taking the default values proposed from SolidWorks program (Fig. 3). The mesh density was selected to dense in the toolholder–epoxy granite contact regions and sparse in other parts of the boring bars. The resultant cutting force applied in tool tip is 52 N (40.5 N in the z -axis, 24.5 N in the y -axis and

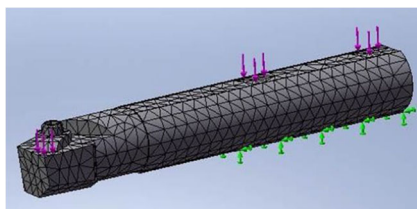


Fig. 3 Finite element model of the boring bar

21.4 N in the x -axis); the clamping force of each bolt of the tool holder is 5592 N, which are determined using Eq. (14) [43].

$$P_{x,y,z} = 10C_p a^x f^y v^n K_p, \tag{14}$$

where a is the depth of cut (mm), f is the feed rate (mm/rev), v is the cutting speed (min^{-1}), x , y , and n are the exponents for specific processing conditions, C_p is a constant for the specific cutting conditions, and K_p is a factor, which takes into account the actual cutting conditions.

The computer analysis includes determination of the tool tip displacement under static loading and calculation of the eigenfrequency at several values of overhang from 40 to 120 mm, since the tool overhang is one of the basic parameters of tool efficiency [17, 18].

2.4 Experimental investigation of boring bars

2.4.1 Static analysis of boring bars

Quality of boring bar under static loading is evaluated by following characteristics: displacement of cutting insert, total displacement of tool tip that is defined by displacement of individual elements, rotation angles of individual elements around the coordinate axes, and by rigid connections of its elements. Taking into account the small linear dimensions of parts of the clamp set and the lack of rigid terminations of basic elements can be neglected by displacement caused by elastic deformations (compression, bending, etc.) of these elements, and assume that all displacement are completely determined by contact deformation.

In the experiment, for boring bars subjected to the cutting force, the relationships “force–displacement” are registered for several cycles of “loading–unloading,” after which the mean value was calculated for each defined displacement for each force. As a result of static experiments on boring bars, the

relationship “force-displacement,” “overhang-logarithmic decrement,” and “amplitude of deformation logarithmic decrement” are obtained for three tool overhangs (40, 80, and 120 mm).

2.4.2 Dynamic characteristics of boring bars

In this section, our studies are conducted to determine the eigenfrequencies of the boring bars, the amplitude of the vibrations with respect to the toolholder at these frequencies, frequency response function of boring bars, damping factor, and compliance of the toolholders. Eigenfrequencies of the boring bars are measured for overhangs 40, 80, and 120 mm by a piezoelectric accelerometer KD-35 attached on the lower side of the cutting edge of the boring bar, multifunctional spectrum analyzer A17-U8, ZETLAB software (Russia), and a personal computer. To determine the damping factor and the compliance, the boring bars were fixed in the tool holder with the overhang of 120 mm. On the toolholder of the boring bars, two piezoelectric accelerometers KD-35 were installed. The analog signal was transmitted through preamplifiers and amplifiers for analog-to-digital converter (ADC). The sampling rate was 50 kHz, and the signal excitation was done three times using the impact hammer PCB Modally Tuned USA No. 4799375 with calculation interval of 10 s. During impacting, in the hammer also an analog signal is produced that is transmitted through the amplifier to the ADC. All signals input to the ADC is converted from analog to digital form and transmitted to a computer for further processing and visualization.

2.4.3 Vibro-acoustic signal investigation of boring bars

The experiments were performed on the machine 16K20VF1 (Russia) for finish turning using boring bars for the overhang 120 mm and the following cutting conditions (spindle speed) $n = 1000$ rpm, (depth of cut) $a = 0.15$ mm, and (feed rate) $f = 0.06$ mm/rev. In the experiment, the AISI 1045 steel with a diameter of 145 mm was used as a workpiece material. Three grooves were produced on the surface of the workpiece in order to deteriorate cutting conditions. The grooves interrupted continuous chips, released the tool tip from its stabilizing effect, and created vibration due to the change in cutting forces while the boring bars were passing the grooves. Such vibrations will help to define better damping properties of boring bars and to study behavior of boring bars during machining of defective parts with deep scratches. Two piezoelectric accelerometer KD-35 were installed on the tool holder so that one of them measured the vibration in vertical direction and the other one in horizontal direction.

2.4.4 Effect of modified boring bars on surface roughness

Carrying out single and full factorial experiments to determine the surface roughness of machined parts using studied boring

bars is the best way to reveal the best designs of modified boring bars and their durability in a real process to judge the possibility of introducing them into production. To determine the effect of cutting parameters in internal machining on the surface quality of the machined part using conventional and modified boring bars, series of experiments were carried out, which were performed on the machine 16K20VF1 (Russia). The Carbide rhombic cutting insert coated with TiC (vertex angle 80°), manufactured by Sandvik Coromant was used as cutting insert. AISI No. 55B and AISI 1045 steel having internal diameter of 145 mm were used as workpiece materials. Machining processes were repeated three times for each cutting tool.

3 Results and discussions

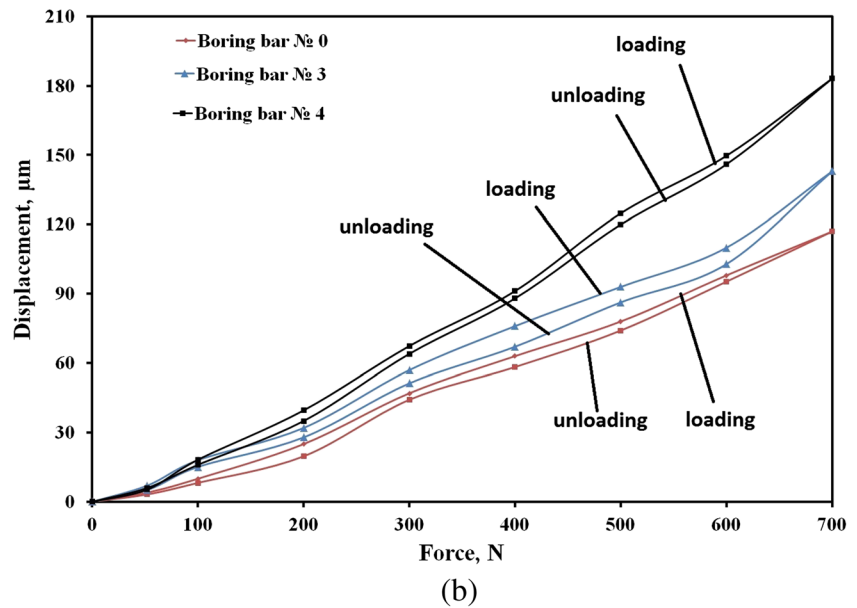
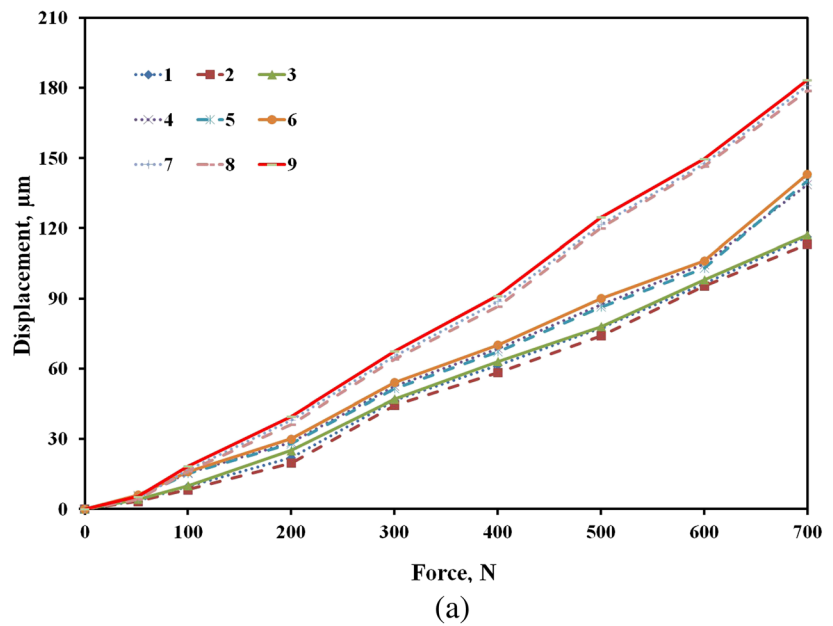
3.1 Static behavior of boring bars

It has been confirmed that boring operation as a commonly used operation, with a slender and long boring bar, is constrained by excessive static deflections and vibrations [40], which cause accelerated wear and tool chip affecting the accuracy and surface finish [31]. The main task of our research into static loading is to determine the relationship between the force and the tool tip displacement. To solve this task, an analytical model, a computer simulation, and several experimental studies were applied. It has been revealed that boring bar Nos. 3 and 4 have a smaller deflection under static force. Figure 4a compares this relationship between “force-displacement” for boring bar Nos. 3 and 4 obtained by analytical model using Eq. (1), computer simulation and experiment. Similar tendencies to those shown in Fig. 4a are observed for other boring tools and overhang lengths. It can be seen that the grooves in the modified bars have reduced their stiffness in comparison with the conventional boring bar. Excessive static deflections may cause the dimensional error, leading to poor surface, short tool life, and tool’s chipping [35]. Comparison of the results obtained by analytical model, computer simulation, and experiment shows that the results are quite similar and the discrepancy is between 7 and 10%. In the static experimental studies, the relationship “force-displacement” was obtained for each tool overhang (40, 80, and 120 mm).

Figure 4b shows this relationship for the overhang of 120 mm, where the curve of the tool tip under loading does not match the curve during the unloading, i.e., the hysteresis loop is obtained, the area that is characterized by the loss of energy, i.e., the toolholder ability to dissipate vibrational energy [29].

Depending on the form of the toolholder, the displacement value and the discrepancy curves tool tip during loading and unloading change. This is due to the difference between the combination of the volume fractions of metal and epoxy

Fig. 4 a Tool tip displacement of the boring bars under static loading for overhang 120 mm. **b** Tool tip displacement of the boring bars under static loading and unloading. 1, analytical (boring bar No. 0); 2, computer simulation (boring bar No. 0); 3, experimental (boring bar No. 0); 4, analytical (boring bar No. 3); 5, computer simulation (boring bar No. 3); 6, experimental (boring bar No. 3); 7, analytical (boring bar No. 4); 8, computer simulation (boring bar No. 4); 9, experimental (boring bar No. 4)



granite, the area of contact, and the moment of inertia of the metal body of toolholder [38]. From the obtained graphs in the form of a hysteresis loop, the damping capacity of the boring bars (logarithmic decrement) as the degree of stability of the boring bar [44] is estimated using Eqs. (15) and (16).

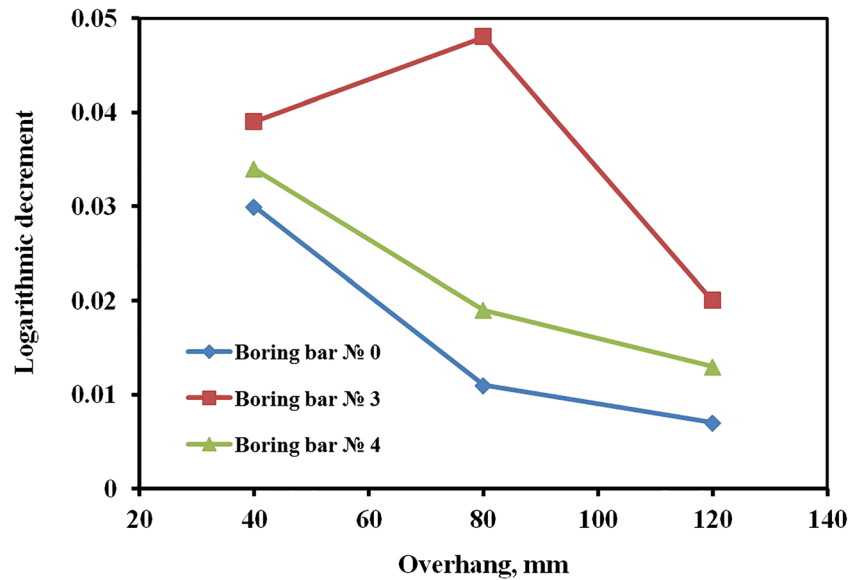
$$\delta = \psi/2, \tag{15}$$

$$\psi = \Delta W/W, \tag{16}$$

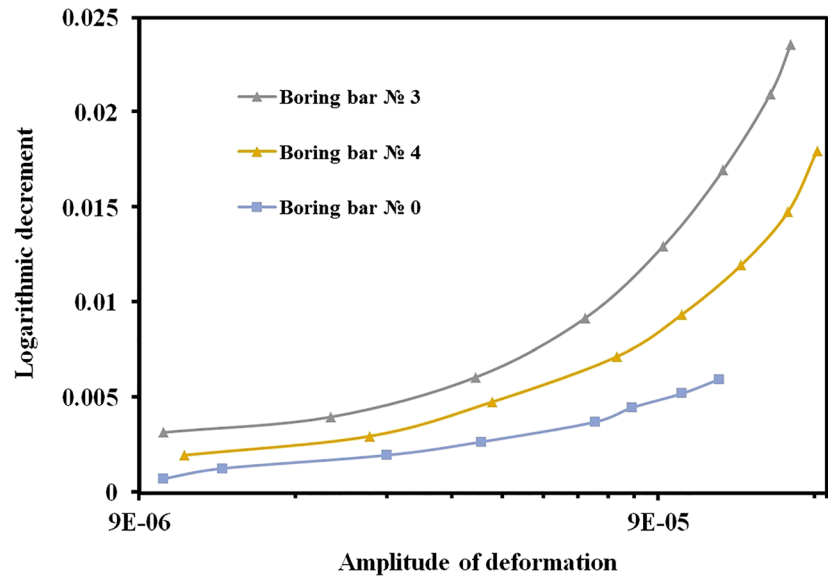
where δ is logarithmic decrement, ψ is coefficient of energy dissipation (damping), ΔW is area between the curve of loading and unloading at the statistical studies, and W is the area between the loading curve and the x -axis.

The calculated data are summarized in the graphs of the relationship between logarithmic decrement, overhang, and the amplitude of deformation shown in Fig. 5a and b. As can be seen from Fig. 5a, as the overhang length for boring bars increases, the logarithmic decrement decreases confirming the results obtained by Ema and Marui [31]. It is revealed that the highest damping capacity and amplitude of deformation occur in boring bar Nos. 3 and 4. This is due to the fact that an increase in the moment of inertia of the metal body decreases the tool tip displacement, which leads to a decrease in the area between the loading curve and the abscissa. An increase in the volume fraction of the composite material in the toolholder leads to an increase in the internal

Fig. 5 **a** The relationship between logarithmic decrement and the tool overhang. **b** The relationship between logarithmic decrement and amplitude of deformation of the cutting tools for the overhang of 120 mm



(a)



(b)

friction, the area between the loading and unloading curves, consequently, to an improvement of the dynamic stiffness of the boring bar, an extension of the stability limits of the machine system [45] and improvement of the vibration and surface finish [29]. Although the type of boring bars with epoxy granite or the overhang length varies, the similar effects of damping capability improvement are evident in comparison with conventional boring bar No. 0.

3.2 Dynamic behavior of boring bars

It is well known that composite materials in a cutting tool play an important role in damping capacity of the tool. Therefore,

many researchers have investigated applications of composite materials to various parts of tooling structures to improve dynamic stiffness and eigenfrequency of machine tool structures [13, 15, 30, 35, 46]. Figure 6a illustrates the relationship between eigenfrequency and tool overhang for 80, 100, and 120 mm. The results revealed that with an increase in the tool overhang, regardless of the geometric and volumetric components of toolholder, the eigenfrequency of the tool is reduced by 2.3 times; the boring bar with epoxy granite decreases eigenfrequency additionally.

Figure 6b compares the eigenfrequency value of boring bar Nos. 0 and 3 obtained by analytical model, computer simulation, and experiment. The differences between the analytical,

Fig. 6 **a** The relationship between eigenfrequency and the tool overhang. **b** Comparison of boring bar eigenfrequencies obtained by analytical model, computer simulation, and experiment. **c** The relationship between amplitude of vibrations and the tool overhang

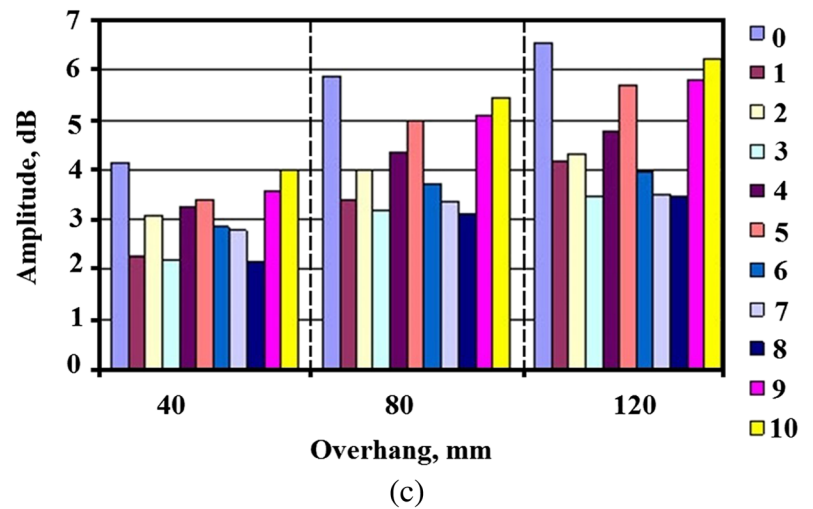
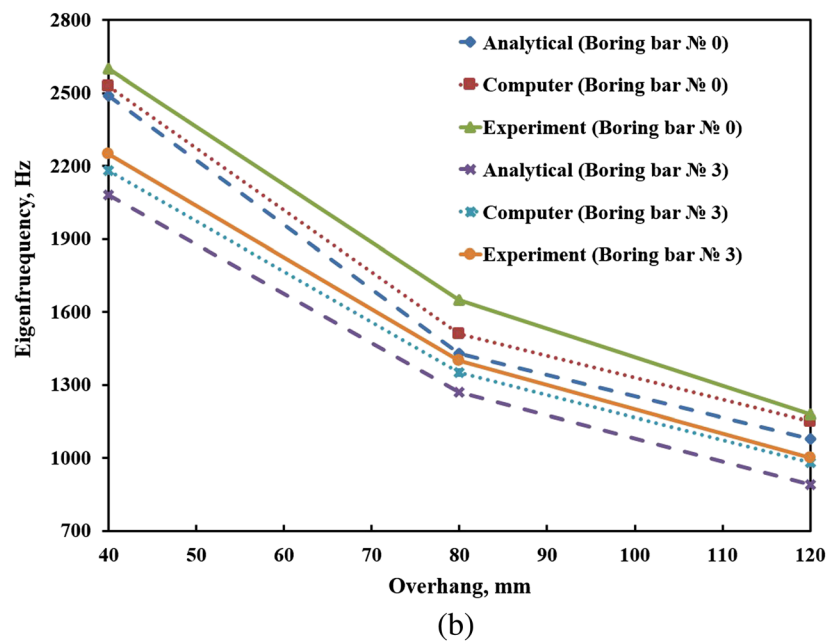
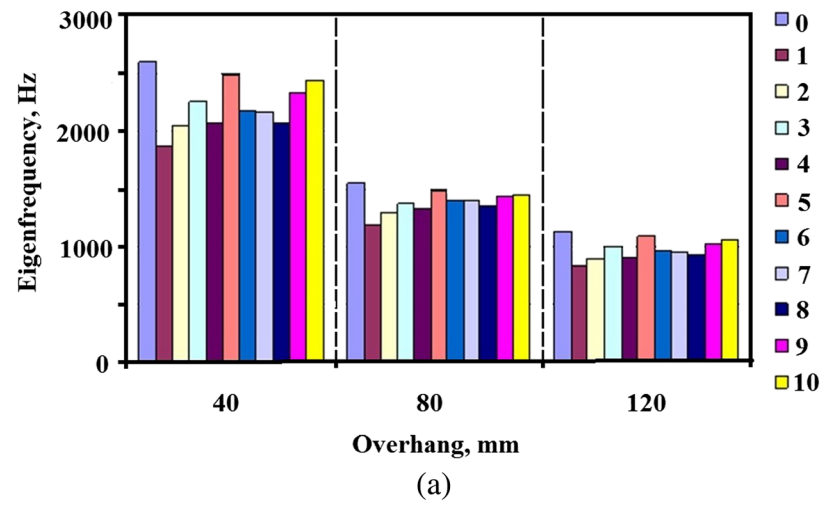


Table 3 Error between analytical, computer simulation, and experimental results of eigenfrequency

Overhang, mm	Percent difference, %					
	E_1	E_2	E_3	E_4	E_5	E_6
40	1.59	4.32	2.72	4.69	3.16	7.85
80	5.44	9.33	3.89	6.10	3.63	9.73
120	6.27	8.84	2.57	8.60	1.02	9.62

computer, and experimental values of the eigenfrequency are evaluated. These differences are less than 10% as shown in Table 3. In Table 3, E_1 and E_4 —percent difference between analytical and computer simulation's results for boring bar Nos. 0 and 3, respectively; E_2 and E_5 —percent difference between analytical and experimental results for boring bar Nos. 0 and 3, respectively; and E_3 and E_6 —percent difference between computer simulation and experimental results for boring bar Nos. 0 and 3, respectively.

The relationship between amplitude of the vibrations and tool overhang is illustrated in Fig. 6c. With increasing the tool overhang from 80 to 120 mm, regardless of the geometric and volumetric components of the tool holder, the amplitude of the vibration of the boring bars relative to the tool holder increases by 40%. This is due to the fact that the unfixed part of the tool increases, because, the moving part of the tool is separated from the fixed part and the distance between them increases. Using the boring bars with epoxy granite reduced the amplitude of the vibration. Lee and Suh [47] observed the same behavior while investigating the effects of stiffness and damping of composite boring bar on the metal cutting ability. They stated that this is related to the fact that the damping property of composite material is higher than that of steel. The highest reduction in the eigenfrequency and amplitude of the vibrations of the boring bars takes place in boring bar Nos. 1, 3, 7, and 8. Boring bar Nos. 3, 5, and 10 have a decrease in the amplitude of the vibrations along Z-axis averaging 30%. To reduce the eigenfrequency, they are a little

inferior to the modified boring bar Nos. 1, 2, 4, and 8. In the next step, the frequency response function of boring bar Nos. 1, 3, 7, 8, and 0 are obtained (Fig. 7). Using the experimental data and the Eqs. (17) and (18), the damping factor and the compliance for two first eigenfrequencies are determined and summarized in Table 4.

$$h(\omega) = \sum_{k=1}^m e_k / \left(1 - (\omega - \omega_{0k})^2 + (2j\xi_k) / \omega_{0k} \right), \quad (17)$$

$$\xi_k = \delta_k / \sqrt{(2\pi)^2 + \delta_k^2}, \quad (18)$$

where ω_{0k} is k -th eigenfrequency without damping; ζ_k is k -th damping factor; e_k is k -th compliance; m is the number of the mode characteristics (eigenfrequency); $j = \sqrt{-1}$, δ_k is k -th logarithmic decrement.

The compliance and damping of the boring bar are two important parameters, because they affect the maximum depth of cut of the boring bar during machining operation, which quantifies the metal cutting stability [33, 38]. The damping factor, hence the dynamic stiffness of the conventional boring bar is much lower than that of the composite boring bar (Table 5), because damping of the composite boring bars is created by the constrained damping of the epoxy granite adhesive between the steel and the inner composite material [40]. The best combination of frequency response function, damping factor, and compliance is achieved for composite boring bar No. 3 at a frequency similar to that of its first resonant frequency. The compliance of this boring bar is 14% less than that of the conventional boring bar No. 0, and the damping factor is five times more than that of the conventional boring bar No. 0. In any case, the stability behavior of boring bars with epoxy granite has been improved compared to the conventional boring bar No. 0 in this work. The eigenvalue of the boring bar can limit the cutting speed of the boring bar. Therefore, if the boring bar possesses a sufficiently high damping ratio, higher cutting speeds would be employed as it was stated by Lee et al. [33]. This could reduce the instantaneous relative vibration between cutting tool and workpiece

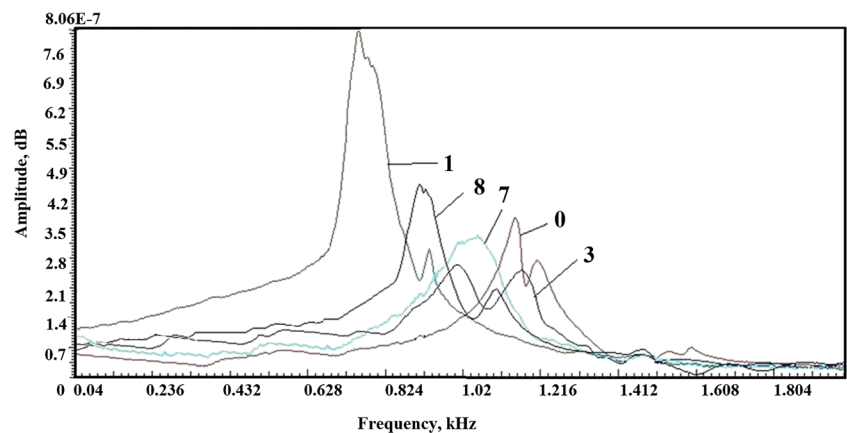
Fig. 7 The frequency response function of the boring bars

Table 4 Damping factor and compliance values of the cutting tools

No.	Modal ratios for first eigenfrequency			Modal ratios for second eigenfrequency		
	Eigenfrequency, Hz	Damping factor, ξ_k	Compliance, Pa ⁻¹	Eigenfrequency, Hz	Damping factor, ξ_k	Compliance, Pa ⁻¹
0	1140	0.0116	0.64	1229	0.0138	0.57
1	820	0.0286	2.49	917	0.0302	2.2
3	991	0.0503	0.55	1000	0.0506	0.49
7	956	0.0448	0.59	994	0.0371	0.61
8	918	0.0491	0.94	976	0.0477	0.86

Table 5 Maximum vibroacceleration of boring bars

		Boring bar				
		No. 1	No. 3	No. 7	No. 8	No. 0
Vibroacceleration (m/s ²)	Vertical	31.7	13.7	54	73	79
	Horizontal	74	56	98	101	132

[4] as well as the waviness of machined surface left by the boring bar at the previous round in a machining process, which are the main physical mechanisms responsible for vibrations [17]. Moreover, Lee et al. [47] claimed that, the metal cutting stability during boring operation without vibration is defined by maximum depth of cut which is proportional to the damping ratio.

3.3 Effect of the boring bars on vibro-acoustic signal during machining process

The quality of the equipment can be assessed by observing the vibro-acoustic signal during machining process,

particularly in intermittent cutting, where the tool repeatedly cuts into hardened surface, which can cause an unstable cutting process, growing chips, large forces, and vibrations leading to machine and cutting tool’s damage [48]. A very small portion of the energy in a machining process with a low damping can cause a large amplitude machine vibration [47]. Figures 8 and 9 depict the vibro-acoustic signals recorded during machining process. It is found that the acceleration amplitude of signal decreased and became more uniform using boring bar with epoxy granite. Such a reduction tendency in vibroacceleration due to the epoxy granite is recognized for all variations in the type boring bars or the overhang lengths.

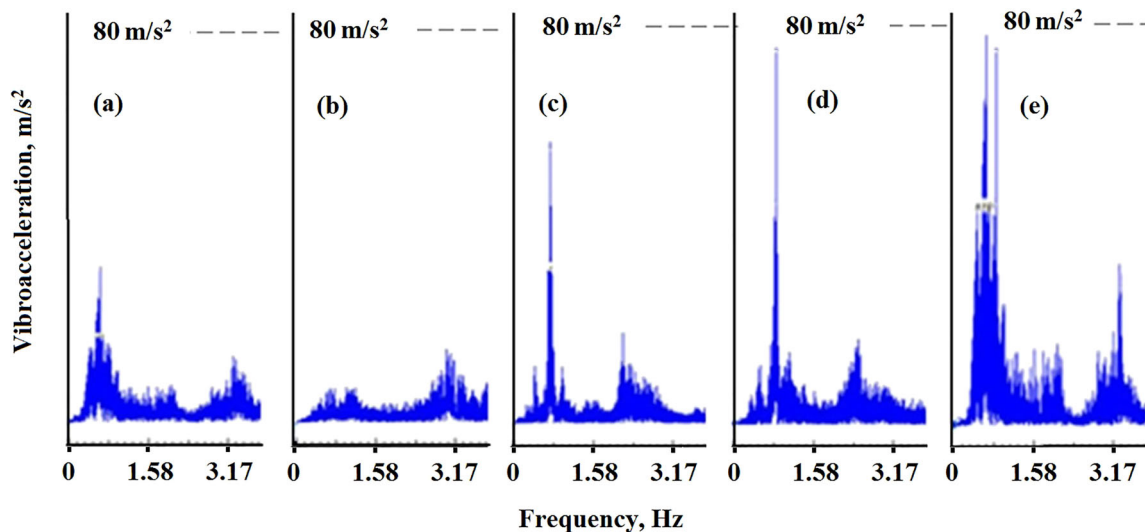


Fig. 8 Vibroacceleration spectra during machining of AISI 1045 with the accelerometers located in vertical direction for boring bars. **a** No. 1. **b** No. 3. **c** No. 7. **d** No. 8. **e** No. 0

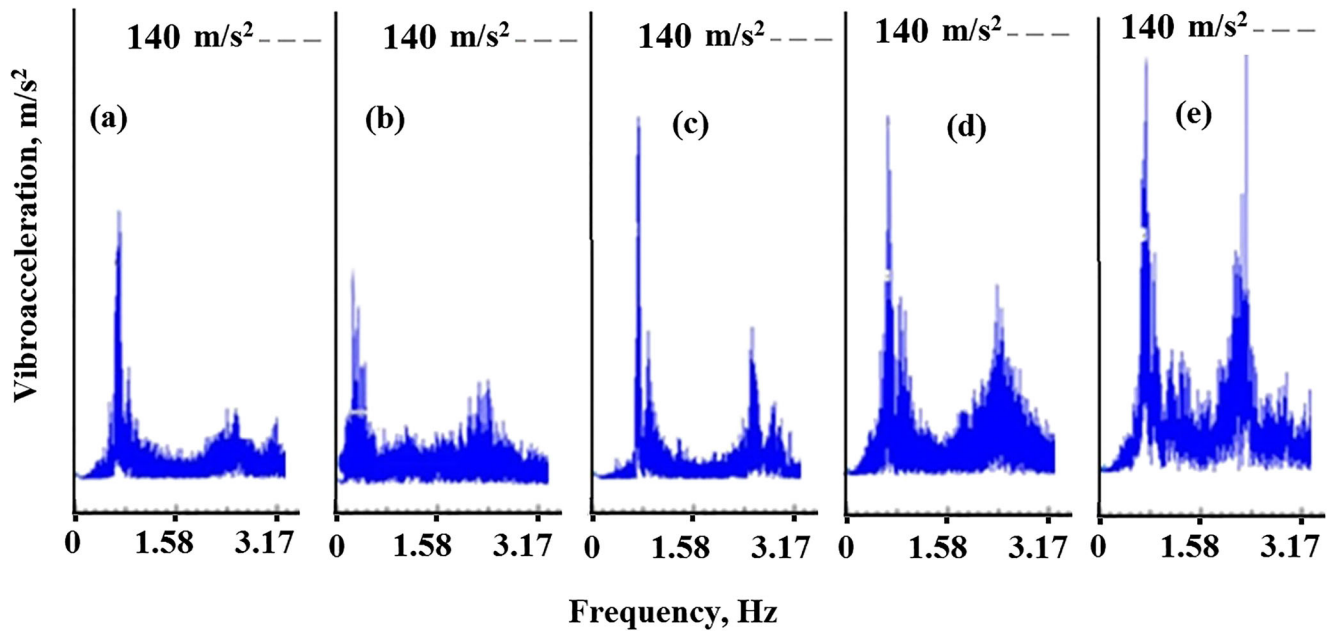


Fig. 9 Vibroacceleration spectra during machining of AISI 1045 with the accelerometers located in horizontal direction for boring bars. **a** No. 1. **b** No. 3. **c** No. 7. **d** No. 8. **e** No. 0

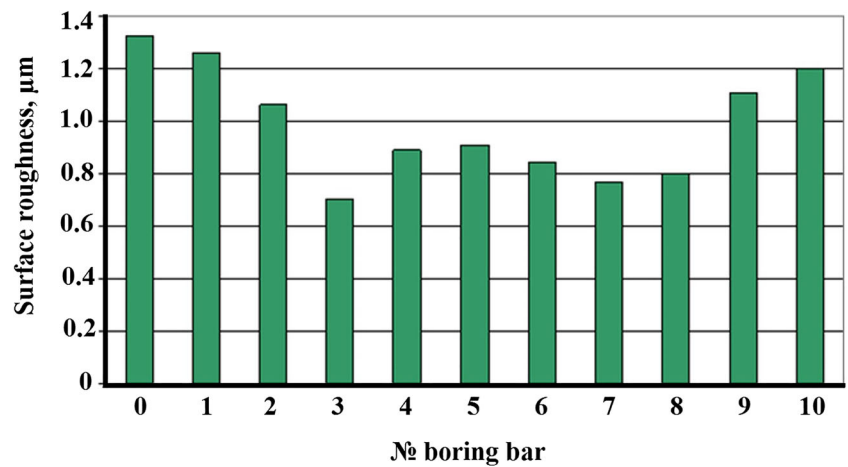
By analyzing, it is observed that the range of acceleration in vertical and horizontal directions for boring bar No. 3 shows the best results (Table 5), i.e., vibroacceleration signal amplitude is small and no dominant harmonics are present (Figs. 8 and 9), which means that the system is stable. Using boring bar No. 3 in machining process reduced the maximum value of vibroacceleration from 79 to 13.7 m/s^2 in vertical direction and from 132 to 56 m/s^2 in horizontal direction. The relation between acceleration level and damping can be explained by the fact that the acceleration level reduces when the damping capacity of the boring bar is increased. Ema and Marui [31] indicated that the damping capacity results from the fact that the boring bar and epoxy granite consume the vibration energy, which is related to the amount of amplitude (acceleration level). For these reasons, the modified boring bars with epoxy granite used in the experiment are considered to be effective

for the suppression of vibration in boring bars. From Figs. 8 and 9, it can be seen that the boring bar Nos. 3, 7, and 8 slightly susceptible to vibrations, which means they have better damping properties compared with boring bar Nos. 0 and 1 confirmed the results obtained in Sections 3.1 and 3.2. It is clear from the results that the vibration of boring bars in the vertical and horizontal directions can be effectively suppressed using boring bars with epoxy granite, by means of which tool wear, tool breakage, and damage of the boring bar affecting surface quality could be avoided [17]. Stepan et al. [49] stated that large vibration amplitudes, in machining operation, cause the loss of contact between the cutting tool and workpiece leading to the self-interrupted cutting. Hence, high material removal rates can be achieved when the dynamic stiffness is high and the hardness is low [1]. The damping capability of composite material results from the boring bar

Table 6 Cutting parameters and their level for single factorial design

Factor	No. of experiment			
	1	2	3	4
Constant factors	$t = 0.15$ mm	$n = 455$ rpm	$n = 455$ rpm	$n = 455$ rpm
	$f = 0.06$ mm/rev	$f = 0.06$ mm/rev	$a = 0.15$ mm	$a = 0.15$ mm
	$L = 120$ mm	$s = 120$ mm	$L = 120$ mm	$f = 0.06$ mm/rev
Variable factors	$n_1 = 287$ rpm	$a_1 = 0.05$ mm	$f_1 = 0.050$ mm/rev	$L_1 = 80$ mm
	$n_2 = 361$ rpm	$a_2 = 0.10$ mm	$f_2 = 0.060$ mm/rev	$L_2 = 100$ mm
	$n_3 = 455$ rpm	$a_3 = 0.15$ mm	$f_3 = 0.075$ mm/rev	$L_3 = 120$ mm
	$n_4 = 569$ rpm	$a_4 = 0.20$ mm	$f_4 = 0.100$ mm/rev	-
	$n_5 = 728$ rpm	$a_5 = 0.25$ mm	$f_5 = 0.125$ mm/rev	-
	$n_6 = 911$ rpm	-	-	-

Fig. 10 Relationship between surface roughness and design of boring bars



with epoxy granite having the heterogeneous structure. Vibration waves pass through the mediums metal and epoxy granite leading to a vibrations suppression, their partial reflection and change of their direction resulting to damping vibration and stabilization of the position of the boring bar, and improvement of the surface finish [38]. Additionally, researches on stability of the system during machining process [1, 9, 11, 50, 51] have shown that the improved dynamic capacity of boring bar increases the stability limit for boring operation.

3.4 Surface roughness evaluation using modified boring bars

In the first step, single factorial experiments were carried out to determine the effect of cutting parameters on the surface roughness. Table 6 shows cutting parameters and their levels for single factorial design. Figure 10 compares the surface roughness (R_a) of the machined part obtained using conventional and modified boring bars at constant cutting speed ($n = 455 \text{ rpm}$), depth of cut ($a = 0.15 \text{ mm}$), feed rate ($f = 0.06 \text{ mm/}$

rev), and overhang ($L = 120 \text{ mm}$), which made it possible to select the best design of damping boring bar for the next series of experiments. As can be seen from Fig. 10, surface roughness values using boring bar Nos. 3, 7, and 8 are less than other ones indicating the higher damping capacities of boring bar Nos. 3, 7, and 8. At the next step, the influence of cutting parameters on the surface roughness using boring bar Nos. 3, 7, and 8 were investigated and compared to the conventional boring bar No. 0 (Figs. 11 and 12). Increase in cutting speed decreases surface roughness while increase in depth of cut, feed rate, and overhang increases surface roughness. Hence, when implementing process planning, measures should be taken to maximize the cutting speed, yet minimize the tool-holder, depth of cut, and the feed rate. However, all composite boring bars improved surface quality compared to the conventional boring bar; it can be seen that using boring bar No. 3 gives better surface quality. Based on the results obtained in single factorial experiments, using modified boring bars during internal machining has improved the surface roughness by 20–40% compared to conventional boring bar. Therefore, using composite boring bars, the risk of crack initiation [52]

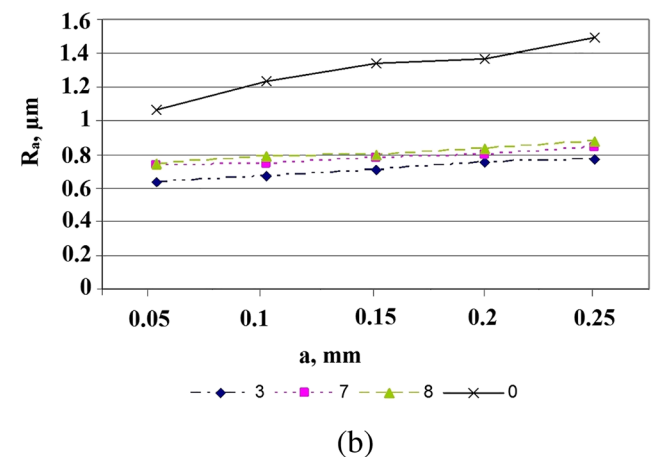
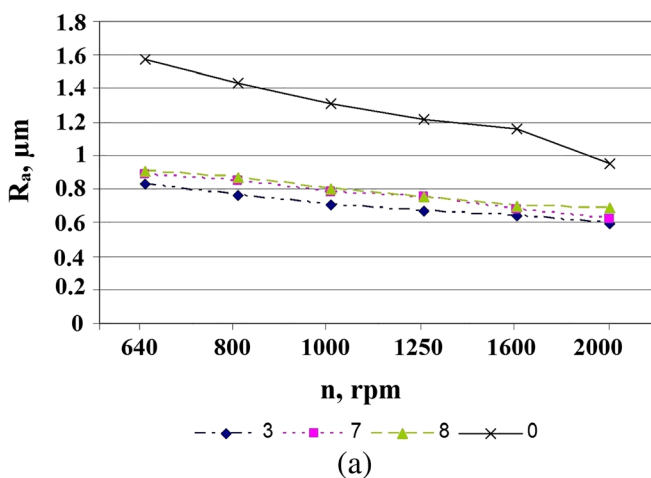


Fig. 11 a Relationship between surface roughness and cutting speed. b Relationship between surface roughness and depth of cut for boring bar Nos. 0, 3, 7, and 8

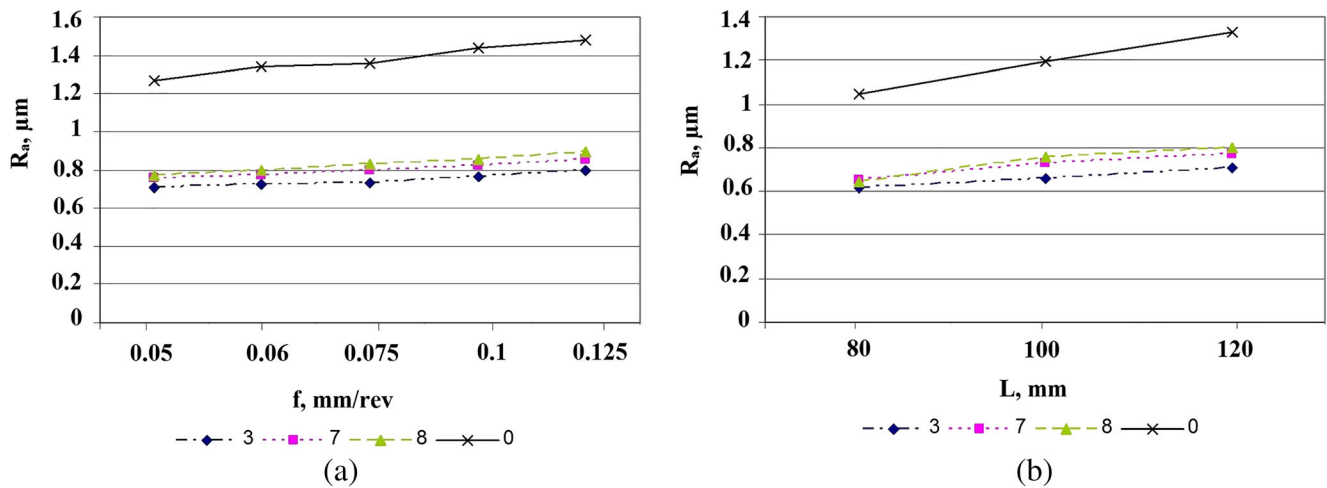


Fig. 12 **a** Relationship between surface roughness and feed rate. **b** Relationship between surface roughness and overhang for boring bar Nos. 0, 3, 7, and 8

can be limited; tool wear and cutting force and tool vibration reduce [53].

The obtained values of roughness do not give a complete picture of the surface layer of the workpiece, as it does not disclose type of obtained surface profile, which directly depends on the ability of the carrying capacity. Therefore, to assess the carrying capacity of the roughness profile, the bearing area curve was obtained, which is a percentage of flat surface created by cutting a line at a defined depth, known as the profile section level. For this purpose, the conventional boring bar (No. 0) and boring bar with the best damping capacity (No. 3) were used for machining of two workpieces made of AISI 1045 steel and AISI No. 55B. Machining process was performed at $n = 1000\text{rpm}$, $a = 0.15\text{ mm}$; $f = 0.06\text{ mm/rev}$; and $L = 120\text{ mm}$. The basis for the construction of bearing area curve is profilogram, which was obtained using profilometer model 170311 (Russia). After analyzing profilogram, the bearing area curve and surface roughness value (R_a) were obtained (Figs. 13 and 14). Figures 13 and

14 show that when machining AISI 1045 steel using the modified boring bar No. 3, the roughness value is less and the bearing area curve are more flat compared to the conventional boring bar No. 0. In the case of machining harder material (AISI № 55B), the surface roughness value decreases, and flatness of bearing area curve increases. A more flat curve of the bearing area curve corresponds to smaller values of roughness with a smooth surface topography.

To identify the best surface roughness value in machining process using conventional and modified boring bars, full factorial experiment (2^4) was carried out. Cutting variables and their levels are shown in Table 7. Material of the workpiece was AISI 1045 steel. As a result of full factorial experiment, mathematical models for surface roughness are obtained (Eqs. (19) and (20)), based on which response surfaces were constructed for both boring bar Nos. 0 and 3 (Figs. 15 and 16). Decrease in cutting speed deteriorates the surface roughness (Figs. 15 and 16). This is related to the fact that at low cutting speeds, the workpiece shear strength appears. In order to

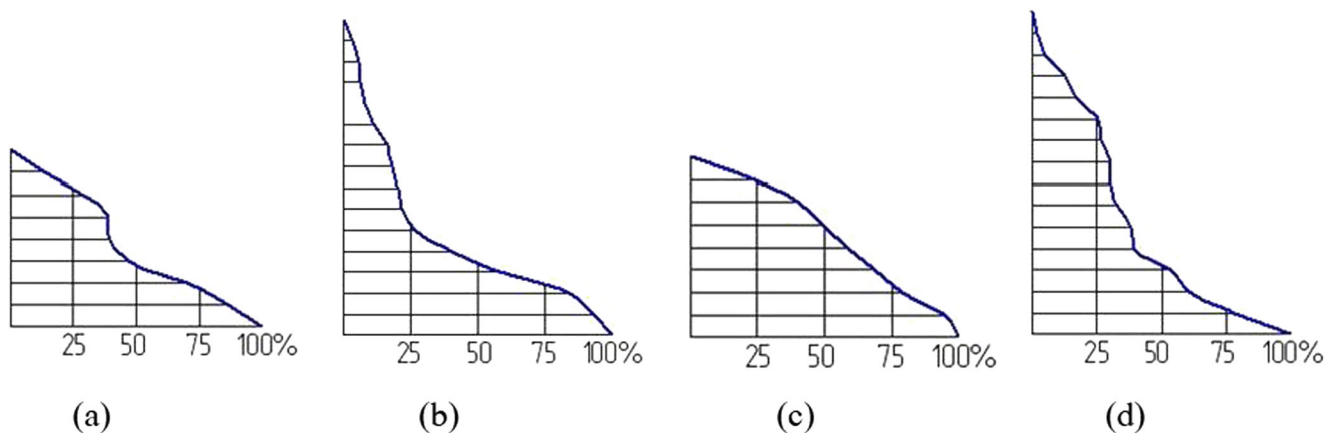
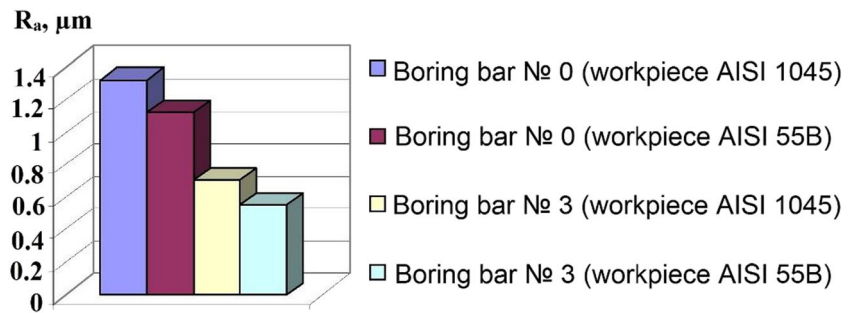


Fig. 13 Bearing area curve. **a** AISI 1045 steel (boring bar No. 3). **b** AISI 1045 steel (boring bar No. 0). **c** AISI No. 55B (boring bar No. 3). **d** AISI No. 55B (boring bar No. 0)

Fig. 14 Surface roughness values during machining of AISI 1045 steel and AISI No. 55B using conventional boring bar (No. 0) and modified boring bar (No. 3)



reduce the shear strength, the heat generation and higher cutting force are required leading to a poor surface roughness [54]. Moreover, Nath and Rahman [55] explained that increase in cutting speed eliminates the formation of built-up-edge leading to an improvement of the surface finish. Increasing in depth of cut decreases surface roughness (Figs. 15 and 16). Bouacha et al [56] claimed that at high depth of cut, the high cutting force is produced leading to an increase in chip interface area and cutting force components affecting the tool life and surface roughness [57].

Figures 15 and 16 show that at lower feed rate, the minimum surface roughness is achieved. The explanation of this phenomenon is that a small distance from peak to valleys on the machined surface improves the surface roughness [58]. Surface roughness decreases when the tool overhang decreases (Figs. 15 and 16) which is related to the fact that at lower overhang, less vibration between cutting tool and workpiece appears which improves surface roughness [38].

For conventional boring bar : R_a

$$= 6.808V^{-0.261}a^{0.211}f^{0.045}L^{0.123}, \tag{19}$$

For boring bar No.3 : R_a

$$= 1.155V^{-0.32}a^{0.05}f^{0.065}L^{0.2}, \tag{20}$$

In addition, it was revealed that use of boring bar filled up with epoxy granite (boring bar No.3) in machining process improves the surface roughness up to 30% compared to conventional boring bar. As it was mentioned before, boring bar, which has less stiffness of structural system, in high loads (high depth of cut, feed rate, and cutting speed) gives poor surface roughness and in lower loads, it is vice versa. Improving the roughness using these boring bars in lower

loads is possible by applying a large volume of damping tool-holder, which has lower load-bearing capacity but it better absorbs vibrations. The damping tool holder also helps to improve the load-bearing capacity of the machined surface.

4 Conclusions

This paper deals with a problem that has a considerable importance for mechanical engineering. This work is focused on the vibration suppression in boring operations by improving structural and technological parameters of boring bars. The effect of the damping capacity of epoxy granite on the performance of boring bar is investigated. The conclusions are as follows:

1. Boring bars filled with epoxy granite, which possesses high damping capacity, with different cross sections, are proposed.
2. The proposed cutting tools are tested during static and dynamic loading using analytical model, computer simulation, and experiments and they were compared. The results indicated that the boring bars with epoxy granite has improved the logarithmic decrement from 0.1 to 0.4 and the eigenfrequency for 15% compared to the conventional boring bar.
3. Best damping characteristics of the studied cross-sections are observed for boring bar No. 3. The compliance of boring bar No. 3 is 14% less than that of the conventional boring bar No. 0, and its damping factor is five times more than that of the conventional boring bar No. 0.
4. The vibro-acoustic signals are also measured during a machining process allowing to select the efficient design of the vibration damping tool with epoxy granite. Vibro-

Table 7 Cutting parameters and their level for full factorial design

Level	Cutting parameters			
	Cutting speed (n), rpm	Feed rate (f), mm/rev	Depth of cut (a), mm	Overhang (l), mm
1	287	0.05	0.05	80
2	911	0.125	0.25	120

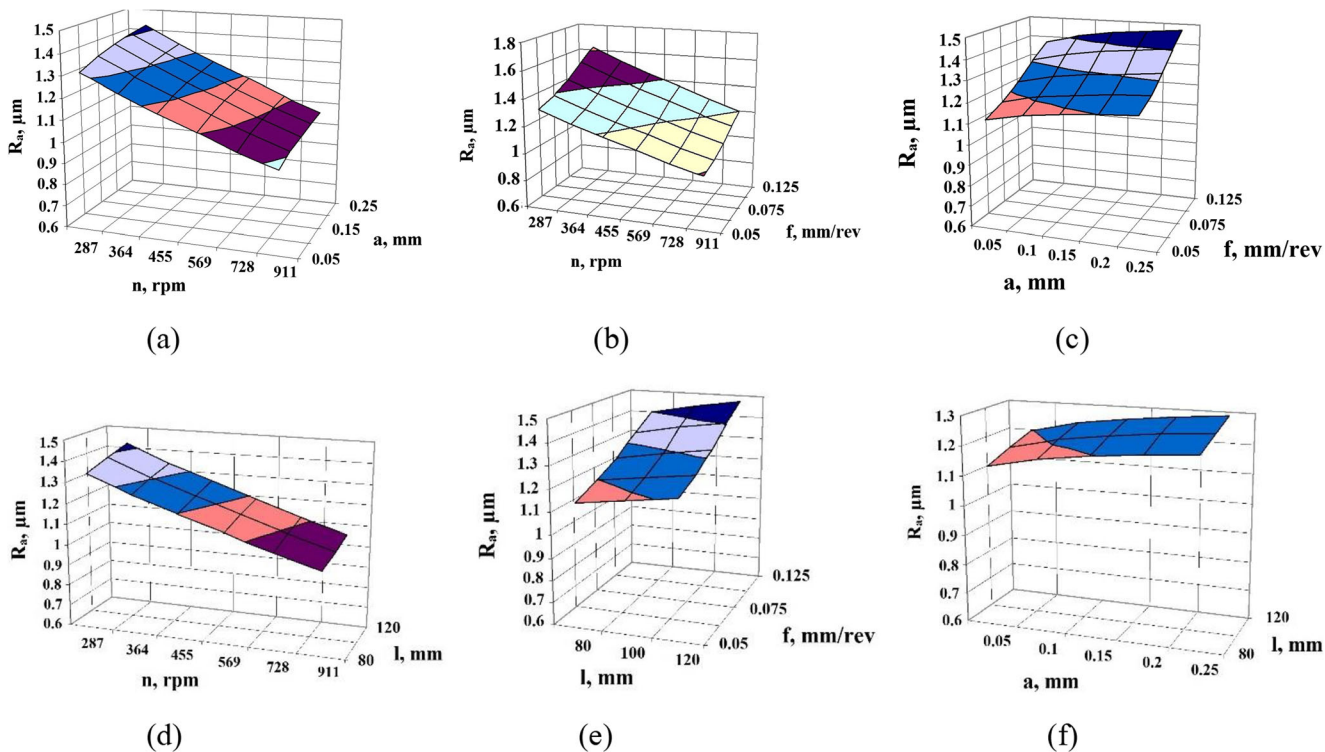


Fig. 15 Relationship between surface roughness and cutting parameters using conventional boring bar No. 0

acoustic studies have shown that using boring bar No.3 filled with epoxy granite can decrease the amplitude from 79 to 13.7 m/s² in vertical direction (in 5.7 times) and from 132 to 56 m/s² in horizontal direction (in 2.5 times)

compared to the conventional boring bar. In a rational combination of stiffness and damping properties, the metal body of the toolholder gives minimal deflection and the vibrations are absorbed by the damping toolholder.

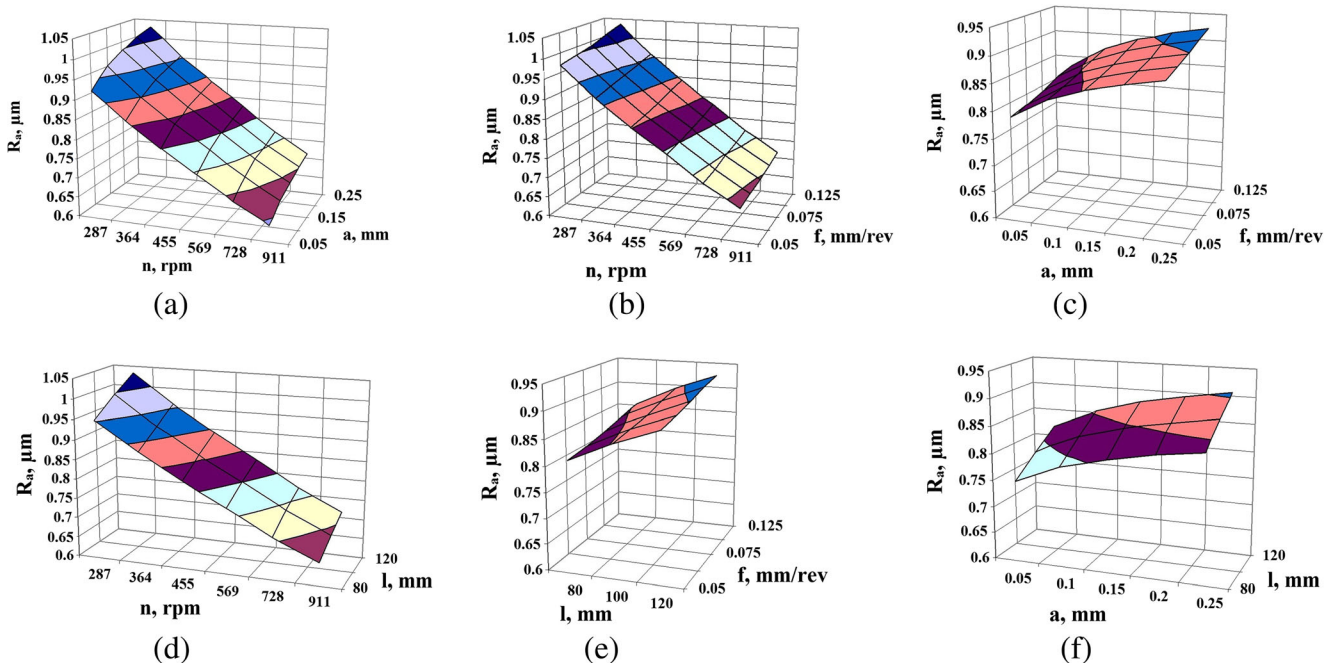


Fig. 16 Relationship between surface roughness and cutting parameters using boring bar No. 3

5. Application of boring bar filled up with epoxy granite in machining process improves the surface quality up to 30% compared to conventional boring bar.

Acknowledgments The publication has been prepared with the support of the «RUDN University Program 5-100.

References

- Tobias SA (1977) Machine tool vibration. China Machine Press, Beijing
- Turkes E, Orak S, Neseli S, Yaldiz S (2012) Decomposition of process damping ratios and verification of process damping model for chatter vibration. *Measurement* 45:1380–1386
- Preś P, Skoczyński W, Jaśkiewicz K (2014) Research and modeling workpiece edge formation process during orthogonal cutting. *Arch Civ Mech Eng* 14:622–635
- Siddhpura M, Paurobally R (2012) Review of chatter vibration research in turning. *Int J Mach Tools Manuf* 61:27–47
- Altintas Y, Weck M (2004) Chatter stability of metal cutting and grinding. *CIRP Ann Manuf Technol* 53(2):619–642
- Taylor FW (1907) On the art of cutting metals. *Trans ASME* 28: 310–350
- Arnold RN (1946) The mechanism of tool vibration in cutting of steel. *Proc Inst Mech Eng* 154:261–284
- Tobias SA, Fishwick W (1958) A theory of regenerative chatter. *Engineer* 205:16–23
- Thusty J, Polacek M (1963) The stability of machine tools against self-excited vibrations in machining. *Inter Res Prod Eng ASME* 465–474
- Smith S, Thusty J (1990) Update on high-speed milling dynamics. *J Eng Ind Trans ASME* 112:142–149
- Merritt H (1965) Theory of self-excited machine tool chatter. *J Eng Ind Trans ASME* 87:447–454
- Altintas Y, Budak E (1995) Analytical prediction of stability lobe in milling. *CIRP Ann Manuf Technol* 44(1):357–362
- Parker EW (1970) Dynamic stability of a cantilever boring bar with machined flats under regenerative cutting conditions. *J Mech Eng Sci* 12(2):107–115
- Zhang GM, Kapoor SG (1987) Dynamic modeling and analysis of the boring machining system. *J Eng Ind* 109(3):219–226
- Rao PN, Rao URK, Rao JS (1988) Towards improved design of boring bars part I: dynamic cutting force model with continuous system analysis for the boring bar performance. *Int J Mach Tools Manuf* 28(1):33–44
- Andren L, Hakansson L, Brandt A, Claesson I (2004) Identification of dynamic properties of boring bar vibrations in a continuous boring operation. *Mech Syst Signal Process* 18:869–901
- Sortino M, Totis G, Prospero F (2012) Development of a practical model for selection of stable tooling system configurations in internal turning. *Int J Mach Tools Manuf* 61:58–70
- Sortino M, Totis G, Prospero F (2013) Modeling the dynamic properties of conventional and high damping boring bars. *Mech Syst Signal Process* 34:340–352
- Akesson H, Smirnova T, Hakansson L (2009) Analysis of dynamic properties of boring bars concerning different clamping conditions. *Mech Syst Signal Process* 23:2629–2647
- Lazoglu II, Atabey F, Altintas Y (2006) Dynamics of boring processes: part III—time domain modeling. *Int J Mach Tools Manuf* 42:1567–1576
- Ozlu E, Budak E (2007) Analytical modeling of chatter stability in turning and boring operations—part I: model development. *J Manuf Sci Eng* 129:726–732
- Ozlu E, Budak E (2007) Analytical modeling of chatter stability in turning and boring operation—part II: experimental verification. *J Manuf Sci Eng* 129:733–739
- Moetafak-Imani B, Yussefian NZ (2009) NZ. Dynamic simulation of boring process. *Int J Mach Tools Manuf* 49:1096–1103
- Qinghua S, Jiahao S, Zhanqiang L, Yi W, Feng X (2015) Boring bar with constrained layer damper for improving process stability. *Int J Adv Manuf Technol* 83(9):1951–1966
- Cook NH (1996) Manufacturing analysis. Addison-Wesley Educational Publisher Inc., United States of America, p 229
- Harris GM (1998) Shock and vibration handbook. McGraw-Hill, United States of America, p 1465
- Blanter MS, Golovin IS, Neuhäuser H, Sinning H-R (2007) Internal Friction in Metallic Materials. Springer Berlin Heidelberg, New York
- Atsushi M, Minetaka M, Iwao Y (2014) Vibration suppression of boring bar by piezoelectric actuators and LR circuit. *CIRP Ann Manuf Technol* 63(1):619–642
- Golovin IS (2006) Damping mechanisms in high damping materials. *Key Eng Mater* 319:225–230
- Nagano S, Koizumi T, Fujii T, Tsujiuchi N, Ueda H, Steel K (1997) Development of a composite boring bar. *Compos Struct* 38(4): 531–539
- Ema S, Marui E (2000) Suppression of chatter vibration of boring tools using impact dampers. *Int J Mach Tools Manuf* 40:1141–1156
- Hwang HY, Lee HG, Lee DG (2004) Clamping effects on the dynamic characteristics of composite machine tool structures. *Compos Struct* 66:399–407
- Lee DG, Hwang HY, Kim JK (2003) Design and manufacture of a carbon fiber epoxy rotating boring bar. *Compos Struct* 60:115–124
- Lee DG, Lee CS, Lee HG, Hwang HY, Kim JW (2004) Novel applications of composite structures to robots, machine tools and automobiles. *Compos Struct* 66:17–39
- Miguelez MH, Rubio L, Loya JA, Fernandez-Saez J (2010) Improvement of chatter stability in boring operations with passive vibration absorbers. *Int J Mech Sci* 52:1376–1384
- Saffury J, Altus E (2009) Optimized chatter resistance of viscoelastic turning bars. *J Sound Vib* 324(1–2):26–39
- Rubio L, Loya JA, Miguelez MH, Fernandez-Saez J (2013) Optimization of passive vibration absorbers to reduce chatter in boring. *Mech Syst Signal Process* 41:691–704
- Rogov VA, Ghorbani S (2015) Research on selecting the optimal design of antivibrational lathe tool using computer simulation. *Proc Inst Mech Eng E-J Pro* 229(3):162–167
- Antonio PF, Flaminio LN (2010) Behavior of granite epoxy composite beams subjected to mechanical vibrations. *Mater Res* 13(4): 497–503
- Nashif AD, Jones DI, Henderson P (1985) Vibration damping. John Wiley and Sons Inc., New York, p 453
- Koch SF, Bauera J, Wagner H, Horsch J, Brecht S, Fleischer J (2014) Characterization of an eigenfrequency adaptable machine tool carriage. *Procedia CIRP* 14:412–417
- Poznyak GG, Rogov VA, Choudhury S (1999) Device for continuously measuring the wear of cutting tool. *STIN* 6:34–35 (in Russian language)
- Kosilova AG, Meshcheryakov RK (1986) Handbook of the technologist for mechanical engineering, Vol. 2, 4 ed. Moscow, Mechanical Engineering
- Choudhury SK, Goudimenko NN, Kudinov VA (1997) On-line control of machine tool vibration in turning. *Int J Mach Tools Manuf* 37(6):801–811
- Archenti A (2011) A computational framework for control of machining system capability, PhD Thesis, KTH Royal Institute of Technology

46. Tewani SG, Rouch KE, Walcott BL (1991) Cutting process stability of a boring bar with active dynamic absorber, vibration analysis. *Anal Commun ASME*:205–213
47. Lee DG, Suh NP (1988) Manufacturing and testing of chatter free boring bars. *CIRP Ann Manuf Technol* 37:365–368
48. Moradi H, Movahhedy MR, Vossoughi G (2012) Dynamics of regenerative chatter and internal resonance in milling process with structural and cutting force nonlinearities. *J Sound Vib* 331:3844–3865
49. Stepan G, Insperger T, Szalai R (2005) Delay, parametric excitation, and the nonlinear dynamics of cutting process. *Int J Bifurcation Chaos* 15(9):2783–2798
50. Hanna NH, Tobias SA (1974) A theory of nonlinear regenerative chatter. *J Eng Ind* 96(1):247–255
51. Rivin E (2000) Tooling structure: interface between cutting edge and machine tool. *CIRP Ann Manuf Technol* 49(2):591–634
52. Davim JP (2011) *Machining of hard materials*. Springer, London
53. Paul PS, Varadarajan AS, Mohanasundaram S (2015) Effect of magnetorheological fluid on tool wear during hard turning with minimal fluid application. *ACME* 15:124–132
54. Bouacha K, Yallese MA, Mabrouki T, Rigal JF (2010) Statistical analysis of surface roughness and cutting forces using response surface methodology in hard turning of AISI 52100 bearing steel with CBN tool. *Int J Refract Met Hard* 28:349–361
55. Nath C, Rahman M (2008) Effect of machining parameters in ultrasonic vibration cutting. *Int J Mach Tool Manu* 48:965–974
56. Dimla DE Sr (2000) Sensor signals for tool-wear monitoring in metal cutting operations—a review of methods. *Int J Mach Tool Manu* 40:1073–1098
57. Benga GC, Abrao AM (2003) Turning of hardened 100Cr6 bearing steel with ceramic and PCBN cutting tools. *J Mater Process Technol* 143–144:237–241
58. Kozlov V, Huang Z, Zhang J (2016) Strength of inserts in titanium alloy machining. *IOP Conf Ser Mater Sci Eng* 124:1–5

Publisher's note Springer Nature remains neutral with regard to jurisdictional claims in published maps and institutional affiliations.